Electron Transfer Reactions of C-shaped Molecules in Alkylated Aromatic Solvents: Evidence that the Effective Electronic Coupling Magnitude Is Temperature-Dependent

Andrew M. Napper, Ian Read, and David H. Waldeck*

Department of Chemistry, University of Pittsburgh, Pittsburgh, Pennsylvania 15260

Ruth W. Kaplan and Matthew B. Zimmt*

Department of Chemistry, Brown University, Providence, Rhode Island 02912

Received: February 18, 2002

The charge separation ($S_1 \rightarrow CT$) and charge recombination ($CT \rightarrow S_1$) rate constants for a C-shaped, donor−bridge−acceptor molecule in the solvent 1,3-di-isopropylbenzene are found to increase, reach a maximum, and then decrease as the temperature is raised from 215 to 360 K. The reaction free energy change for the charge separation and charge recombination processes are determined from the ratio of the two rate constants. The charge separation and the charge recombination rate constants also display a maximum when plotted against the experimental reaction free energy (Marcus plot). This behavior can be quantitatively modeled in two different ways: (i) using a small and temperature-independent value of the solvent reorganization energy, which results in transitions between the Marcus normal and the Marcus inverted region as the reaction free energy changes with temperature and (ii) allowing a decrease in the magnitude of the donor−acceptor electronic coupling at elevated temperatures. The latter explanation is shown to be more consistent with current information regarding the magnitude and temperature dependence of the solvent reorganization energy in alkylaromatic solvents and with known examples of the Marcus inverted region.

I. Introduction

The requirements for fast electron-transfer processes are favorable Franck−Condon factors and significant electronic coupling between the donor and acceptor groups. Electronic coupling magnitudes in electron-transfer systems vary from thousands of wavenumbers, e.g., for contact ion pairs,[1] to hundredths of wavenumbers for donor and acceptor groups separated by tens of angstroms, e.g., in proteins and glasses.[2] Different methods are used to determine coupling magnitudes from experimental data. Systems with moderate couplings (10−200 cm^{-1}) often exhibit charge transfer (CT) absorption and/or CT emission bands. Analysis of these bands' transition intensities provides values of the donor−acceptor electronic coupling.[1,3] For systems with smaller donor−acceptor couplings, CT transitions are usually too weak to detect and analyze. The electronic coupling magnitudes in "weakly coupled" systems may be determined through analysis of electron-transfer rate constants, once the appropriate Franck−Condon factors have been determined or estimated. Despite the indirect nature of this approach, a number of such investigations have successfully identified relationships between the electronic coupling magnitude and the underlying molecular structure and/or properties of the medium between the donor and acceptor groups.[4]

It has long been appreciated that the structure of the medium between the donor and acceptor groups influences the rates of electron transfer. Less widely recognized is the important role that dynamics can exert. For many electron transfer reactions, the structure of the medium through which the electron tunnels is dynamic. Theoretical investigations have indicated that intervening medium motions, including vibrations, librations, conformational changes, and diffusion of mobile components, can significantly modulate donor−acceptor electronic coupling magnitudes.[5] The size of the coupling magnitude fluctuations depends on the amplitudes of the medium motions and the details of the electronic coupling pathways. A dramatic manifestation of the influence of dynamics is "conformational gating",[6] which has been observed for protein and intramolecular electron transfer reactions. This phenomenon occurs in long-range electron transfer systems when the electron transfer rates for a subset of the thermally accessible conformations is fast relative to the transfer rates in the most populated conformations. The observed transfer rate is influenced by the kinetics of interconversion among conformations. Larger coupling magnitudes in the "fast" conformations can contribute to the "gating" effect. The variation of coupling magnitude with conformation constitutes a break down of the Condon approximation.

It is difficult to quantify the influence of structural fluctuations on coupling magnitudes in electron transfer systems with small electronic couplings because electron transfer rates, not coupling magnitudes, are the experimental observables. Extraction of the coupling magnitude from experimental rate data requires reliable evaluation of activation barriers, nuclear factors, and solvation. Generally, it is difficult to ascertain the existence and/or magnitude of coupling fluctuations from such an analysis. In those intramolecular electron transfer systems where a structurally rigid bridge connects the donor and acceptor, structural distortions of the bridge and coupling magnitude fluctuations are likely small.[7] For intra- and intermolecular electron-transfer systems in which the structure of the intervening medium fluctuates significantly, the donor−acceptor electronic coupling may also fluctuate significantly. Hence, the electronic coupling,

* To whom correspondence should be addressed.

10.1021/jp0204455 CCC: $22.00
Published on Web 04/17/2002

CHART 1: Molecular Structures of the Electron Transfer Molecules 1, 2, and the Solvent 1,3-Di-isopropylbenzene.

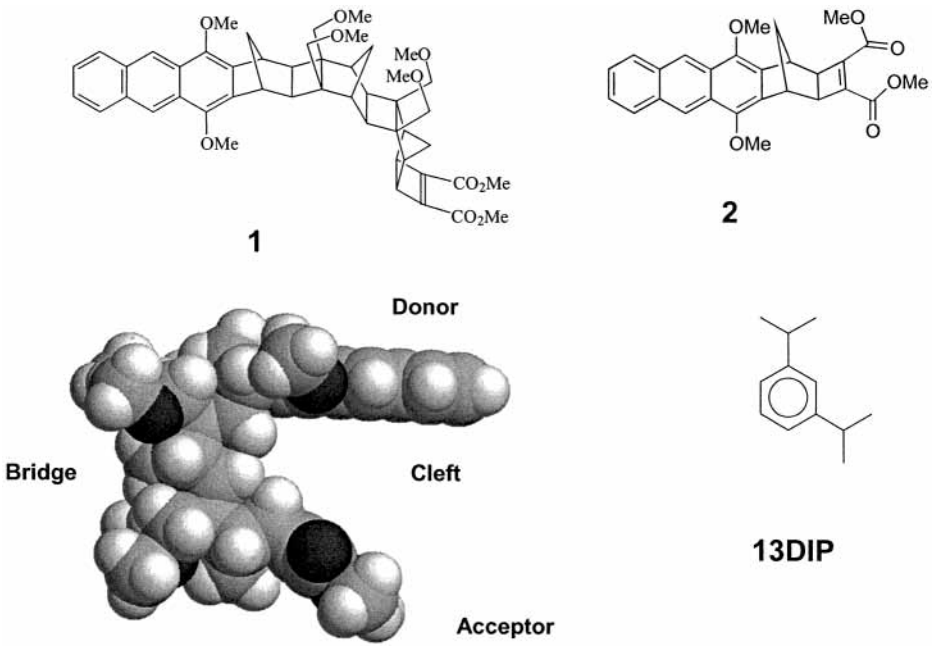

extracted from rate constant analysis, represents a (dynamically) averaged electronic coupling matrix element, or an "effective" coupling magnitude. As the majority of investigations are not posed to investigate these effects, little evidence for or characterization of medium induced fluctuations of the electronic coupling is available.

Recent investigations of some highly curved donor−bridge−acceptor molecules indicate that their electronic coupling may derive from "pathways" constituted by solvent molecules.[8] The coupling magnitudes in these systems are influenced by the solvent molecules' electronic structure, size, shape, and the size of the solvent accessible gap between the donor and acceptor groups.[8] Calculations suggest that the magnitude and sign of the electronic coupling mediated by solvent molecules varies significantly with the latter's placement and orientation relative to the donor and acceptor. Consequently, the relatively rapid and unconstrained motions of the solvent molecules should give rise to a fluctuating electronic coupling magnitude.[5e] Additionally, environmental variables that alter the solvent dynamics and/or accessible conformations, e.g., pressure[9] or temperature, may influence the "effective" value of the electronic coupling that is determined through analysis of rate constant data. As is true for systems exhibiting conformational gating,[6] fluctuation of the donor−acceptor coupling associated with solvent motion constitutes a breakdown of the Condon approximation. Previous investigations have provided some evidence that solvent-mediated electronic coupling magnitudes are temperature-dependent.[10] This investigation reports data that indicate a strong temperature dependence of the solvent-mediated, donor−acceptor electronic coupling for a C-shaped molecule, **1** (Chart 1). The evidence of temperature-dependent coupling is particularly compelling for extensively alkylated aromatic solvents.

Compound **1** (see Chart 1) juxtaposes a dimethoxyanthracene donor and a cyclobutene diester acceptor on opposite sides of a 7 Å cleft that is accessible to solvent molecules. The electron-transfer dynamics of **1** have been investigated in highly polar,[8b] alkylated-aromatic,[8c,10] and halo-aromatic solvents.[11] The electronic coupling magnitude determined for **1** in each solvent depends on the solvent's electronic energy levels and its three-dimensional structure.[8,10,11] The electron-transfer reactions of **1** in alkylated benzene solvents afford an unusual opportunity for in-depth investigation of the factors that control rate constants. The reaction free energy, $\Delta_r G$, is almost zero for electron transfer from the lowest energy, singlet-excited state (S_1) of the anthracene donor to the acceptor. An equilibrium between the anthracene S_1 excited state and the charge separated state influences the fluorescence dynamics and allows determination of all three electron-transfer rate constants after the $S_0 \rightarrow S_1$ excitation:[8c] the charge separation, electron-transfer rate constant for conversion of the anthracene S_1 state to the charge separated state, k_{for}; the charge recombination rate constant for conversion of the charge separated state back to the anthracene S_1 state, k_{back}; and the charge recombination rate constant that converts the charge separated state to the anthracene S_0 state, k_{rec}.[12] The free energy gap between the anthracene S_1 excited state and the charge separated state is evaluated experimentally from the first two of these rate constants.

The temperature dependence of the charge separation and charge recombination rate constants of **1** vary dramatically depending on the structure of the alkyl benzene solvent. In benzene, the charge separation rate constant, k_{for}, decreases and the charge recombination rate constant, k_{back}, increases as the temperature is increased. By contrast, k_{for} and k_{back} in 1,3,5-tri-isopropylbenzene both increase as the temperature increases. The rate constants k_{for} and k_{back} for **1** in 1,3-di-isopropylbenzene exhibit more complex behavior, first increasing and then decreasing as the temperature is raised. The nonmonotonic temperature dependence of k_{for} and k_{back}, along with the availability of $\Delta_r G(T)$ data, provide significant constraints on kinetic models used to interpret these rate data. In particular, two possible explanations for the observed rate constant behavior of **1** in 1,3-di-isopropylbenzene can be identified. First, the temperature dependence can be explained by a decrease of the effective electronic coupling magnitude with increasing temperature. Second, the temperature dependence could result from a small and temperature-independent value of the solvent reorganization energy, which, in conjuction with the temperature dependence of $\Delta_r G$, moves the charge separation and recombination reactions, k_{for} and k_{back}, between the Marcus normal and inverted regions. Both interpretations can quantitatively

reproduce the observed data for **1** in 1,3-di-isopropylbenzene and are consistent with the models used to predict electron transfer rate constants. As discussed later in the manuscript, the combination of these data with earlier data in alkylbenzene solvents argues strongly for the first explanation, a temperature dependence of the electronic coupling magnitude.

This manuscript describes the determination and analysis of the electron-transfer rate constant for **1** in 1,3-di-isopropylbenzene solvent. Data collection, rate constant determinations, and determination of the reaction free energy are described in the next section. The two explanations for the temperature dependence of the rate constants are developed in the third section. They differ significantly in the magnitude and temperature dependence of the solvent reorganization energy, $\lambda_S(T)$. The fourth section describes the evidence for and against the two explanations and discusses the implications of these findings for solvent and temperature-dependent rate constants observed earlier. Although it is not possible to reject unambiguously either explanation, the explanation based on a temperature dependence of the effective electronic coupling magnitude is more consistent with prior experimental and theoretical results.

II. Data, Rate Constant, and $\Delta_r G$ Determinations

The preparation of **1** was reported elsewhere.[13] Solutions of **1** were prepared with an optical density of ca. 0.05 at the laser excitation wavelength, 375 nm. The solvent 1,3-di-isopropylbenzene (98%) was purchased from Aldrich. The solvent was dried with anhydrous magnesium sulfate, filtered, and then fractionally distilled using a vigreux column. The purified fraction was used immediately to prepare the sample. Each sample solution was freeze−pump−thawed a minimum of three times. The samples were back-filled with argon to reduce solvent evaporation at the higher temperatures.

Excitation of the sample was performed at 375 nm by the frequency-doubled cavity-dumped output of a Coherent CR-599−01 dye laser using LDS750 (Exciton) dye, which was pumped by a mode-locked Coherent Antares Nd:YAG laser. The dye laser pulse train had a repetition rate of ca. 300 kHz. Pulse energies were kept below 1 nJ, and the count rates were kept below 3 kHz. All fluorescence measurements were made at the magic angle. Other specifics of the apparatus have been reported elsewhere.[14] Instrument response functions were measured using a sample of colloidal $BaSO_4$ in glycerol. Fluorescence decays were fit to a sum of two exponentials (the decay law was convolved with the measured instrument function) using the Marquardt−Levenberg nonlinear least squares algorithm. Figure 1 shows a fluorescence decay for **1** in 1,3-di-isopropylbenzene at 290 K, the calculated best-fit, biexponential decay curve, the impulse response, and the fit residuals. For temperatures above 260 K, the sample cuvette was placed in an aluminum block whose temperature was controlled by a NESLAB RTE-110 chiller. Temperatures were measured using a type-K thermocouple (Fisher-Scientific), accurate to within 0.1 °C. Slush baths were used for the lower temperature points: 247 K (*o*-xylene/liquid N_2), 240 K (chlorobenzene/liquid N_2), 235 K (acetonitrile/liquid N_2), and 218 K (chloroform/liquid N_2). The slush bath temperatures varied by ±2 K from the stated temperature.

Kinetic and Thermodynamic Analyses. Photoexcitation of the anthracene donor moiety creates a locally excited state (S_1 or LE) whose energy is similar to that of the charge separated state in 1,3-di-isopropylbenzene solvent. The inset to Figure 1 shows the kinetic scheme that is used to describe the kinetics following formation of the locally excited state by the light

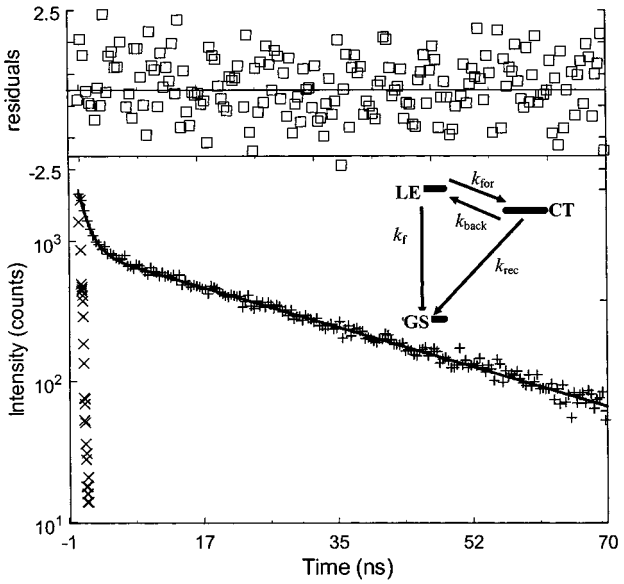

Figure 1. Fluorescence decay for **1** in 1,3-di-isopropylbenzene at 290 K and the best fit to the data (solid line hidden by the raw data). The impulse response function (×) and the residuals (□, at top) are also shown. The fitted curve gives rate constants of 814 ps (68%), 17.7 ns (32%), and a χ^2 of 1.08. The inset shows an energy level diagram for the kinetics.

pulse. There are four unknown rate constants. The intrinsic decay rate constant of the locally excited state, k_f, is obtained from the LE decay kinetics of an analogue to molecule **1** that has no electron acceptor. Fitting the time-resolved fluorescence decay of **1**'s LE state to a biexponential form provides three additional parameters: a fast rate constant, a slow rate constant, and the amplitude fraction of the fast decay. The electron-transfer rate constants k_{for}, k_{back}, and k_{rec} are calculated using the fit parameters that reproduce the time-resolved fluorescence decay.[15] The Gibbs free energy of the charge separation reaction is determined at each temperature from the ratio of the forward and back rate constant, (eq 1)

$$\Delta_r G = -RT \ln(k_{for}/k_{back}) \quad (1)$$

The availability of experimental $\Delta_r G$, at each temperature, and of the internal reorganization energy parameters (vide infra) make it feasible to interpret the temperature-dependent rate constant data in terms of only two parameters: the solvent reorganization energy and the donor−acceptor electronic coupling.

III. Rate Constant Temperature Dependence and Possible Explanations

Figure 2 summarizes the temperature-dependent rate constant and $\Delta_r G$ data. Panel A displays the temperature dependence of the charge separation and charge recombination rate constants for molecule **1** in 1,3-di-isopropylbenzene. Starting at 218 K, 8° above the solvent's melting point, both the charge separation and charge recombination rate constants increase upon increasing the temperature. The charge separation rate constant, k_{for}, reaches a maximum near 270 K and then decreases sharply at higher temperatures, dropping more than 20-fold by 356 K. The charge recombination rate constant, k_{back}, increases up to 320 K and then decreases 2-fold by 356 K. The maximum rate constants for the charge separation and charge recombination reactions are nearly equal, $\sim 9 \times 10^8$ s^{-1}. Panel B presents the experimental $\Delta_r G$ for the charge separation reaction as a function

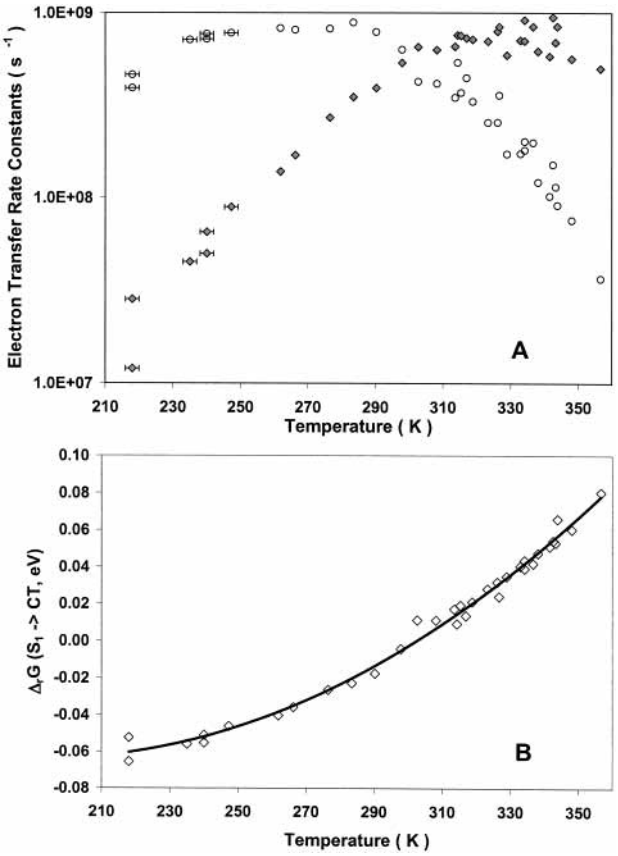

Figure 2. (Panel A) Charge separation (k_{for}, ○) and charge recombination (k_{back}, ◆) rate constants for molecule **1** as a function of temperature in 1,3-di-isopropylbenzene. Panel B plots the free energy change for charge separation (k_{for}, ◇) as a function of temperature for **1** in 1,3-di-isopropylbenzene. The solid line represents a best fit of the data to a quadratic equation.

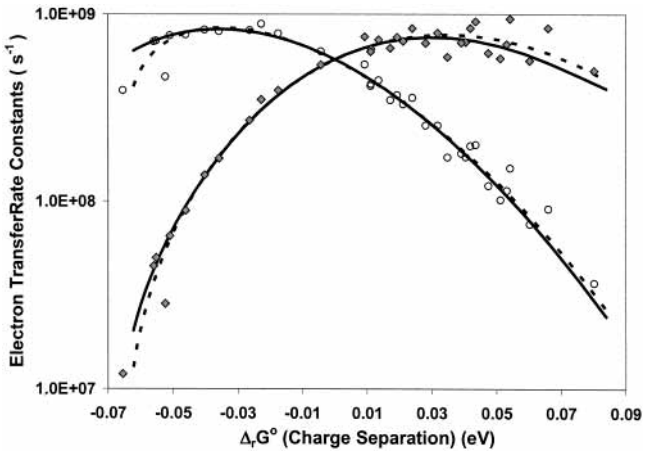

Figure 3. Plots of the charge separation (k_{for}, ○) and charge recombination (k_{back}, ◆) rate constants versus the free energy change for charge separation. To minimize overlap, both plots use the charge separation $\Delta_r G$ as the abcissa. The solid lines were calculated using eq 2 assuming $|V| = 2.25$ cm^{-1} and $\lambda_S = 0.033$ eV. The dashed lines were calculated using the parametrized Matyushov model to predict $\lambda_S(T)$ and the regression estimates of $|V(T)|$ (see text).

of temperature. The free energy of charge separation varies nearly linearly from 280 to 350 K. However, as the temperature approaches the freezing point of the solvent, $\Delta_r G$ changes less steeply with temperature. The solid line shows a fit to the full temperature dependence of $\Delta_r G$ that is obtained with a quadratic expression. This fit is used later to aid in the analysis of the rate data.[16]

Semi-log plots of electron-transfer rate constant versus reaction free energy have been used to determine solvent reorganization energy and electronic coupling magnitudes. For **1**, the logarithms of k_{for} and k_{back} increase, plateau, and then decrease in a plot versus $\Delta_r G$ for the charge separation step (Figure 3). This shape suggests that k_{for} and k_{back} both span the Marcus normal and inverted regions and that the solvent reorganization energy is very small (vide infra). In a conventional Marcus plot, the temperature and solvent reorganization energy for all points are held as constant as possible. In Figure 3, however, the temperature for each data point varies from 218 (left side) to 356 K (right side). As a result, the variation of $\Delta_r G$ (abscissa) is attended by significant variation of $k_B T$ and, possibly, of the solvent reorganization energy and the electronic coupling. These variations must be considered in any interpretation of the rate constant plots in Figures 2 and 3 (vide infra).

The temperature dependence of the charge separation and recombination rate constants may be simulated using a semiclassical formulation[17] for the electron-transfer rate constant (eq 2)

$$k_{et} = \frac{4\pi^2}{h}|V|^2 \frac{1}{\sqrt{4\lambda_S \pi k_B T}} \times \sum_{n=0}^{\infty} \exp(-S)\left(\frac{S^n}{n!}\right) \exp\left[-\frac{(\Delta_r G + \lambda_S + nh\nu)^2}{4\lambda_S k_B T}\right] \quad (2)$$

In this equation, $|V|$ is the donor−acceptor electronic coupling, λ_S is the solvent reorganization energy, $h\nu$ is the quantized mode energy spacing, and S is the ratio of the internal reorganization energy, λ_V, to the quantized mode energy spacing, $S = \lambda_V/h\nu$. The quantity S is assumed to be temperature independent. Estimates of λ_v (0.39 eV) and $h\nu$ (0.175 eV) were previously determined using a combination of quantum chemistry calculations and CT emission spectra from related molecules.[18] Given these values for the internal reorganization parameters and the experimental values of $\Delta_r G$ at each temperature (Figure 2B), only the magnitude and temperature dependence of λ_S and $|V|$ may be "adjusted" to reproduce the experimental data. The extensive curvature of the k_{for} and k_{back} versus $\Delta_r G$ plots places significant constraints on the magnitude and temperature dependence of the solvent reorganization energy and/or of the electronic coupling. As discussed below, two possible explanations for the highly curved plots of k_{for} and k_{back} versus temperature (i.e., versus reaction free energy) have been identified.

The experimental k_{for} and k_{back} rate constants at each temperature establish a parametric relationship between the two unknown parameters in eq 2: the solvent reorganization energy and the electronic coupling. At 297 K, the temperature at which $\Delta_r G = 0$, the charge separation, and charge recombination rate constants are equal, and only the $n = 0$ term in eq 2 makes significant contributions to either rate constant. The electronic coupling may be expressed as a simple function of the solvent reorganization energy, the temperature, and the rate constants by rearranging eq 2. Figure 4 displays this relationship between $|V|$ and λ_S for **1** in 1,3-di-isopropylbenzene at 297 K, with $k_{for} = k_{back} \sim 5.8 \times 10^8$ s^{-1}, and shows that the electronic coupling increases monotonically as λ_S increases. A previous study of solvent-mediated, donor−acceptor electronic coupling for **1** determined that $|V| = 6$ cm^{-1} in isopropylbenzene (cumene) and $|V| = 1$ cm^{-1} in 1,3,5-tri-isopropylbenzene.[10] Furthermore,

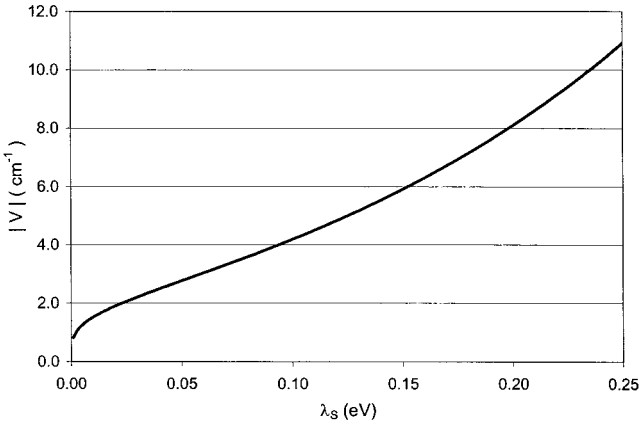

Figure 4. Correlation between $|V|$ and λ_S for **1** derived from the experimental transfer rate constant at 297 K, where $\Delta_r G = 0$ eV.

it was found that an increase in the alkyl substitution at the periphery of the benzene ring caused a systematic decrease of the magnitude of solvent-mediated coupling for **1**.[8c] Accordingly, the electronic coupling mediated by 1,3-di-isopropylbenzene for **1** is expected to lie between the values in cumene and tri-isopropylbenzene, i.e. between 6 and 1 cm^{-1}, respectively. Using the range defined by these couplings, Figure 4 indicates that the solvent reorganization energy in 1,3-di-isopropylbenzene at 297 K lies between 0.15 and 0.0 eV, respectively. The experimental values of $\Delta_r G$ for charge separation in 1,3-di-isopropylbenzene vary, with temperature, between -0.07 and 0.08 eV. Thus, the charge separation reaction could lie in the Marcus normal region (if $\lambda_S > 0.09$ eV) or span the normal and inverted regions ($\lambda_S < 0.06$ eV).

By assuming a specific, *temperature independent* value of the electronic coupling, eq 2 may be used to determine the value of λ_S that is required at each temperature to reproduce the experimental rate constants. Figure 5 displays $\lambda_S(T)$, calculated in this manner, for two assumed values of the electronic coupling: 2.25 cm^{-1} (panel A) and 6.0 cm^{-1} (panel B). For the assumed value of $|V| = 2.25$ cm^{-1}, the extracted λ_S has a mean value of 0.033 ± 0.007 eV and exhibits a weak, positive temperature dependence, <0.1 meV/K. If λ_S for **1** in 1,3-di-isopropylbenzene is this small and without significant temperature dependence, the charge separation reaction lies in the Marcus inverted region at temperatures below 270 K, and the charge recombination reaction lies in the Marcus inverted region at temperatures above 330 K. The solid lines in Figure 3 display the temperature dependence of k_{for} and k_{back} predicted using $\lambda_S = 0.033$ eV, $|V| = 2.25$ cm^{-1} and $\Delta_r G$ obtained from the data in Figure 2B. The calculated curves reproduce the data well. Using the larger assumed value of $|V| = 6.0$ cm^{-1}, the λ_S values extracted with eq 2 (Figure 5B, circles) exhibit a U-shaped temperature dependence with a value at 297 K of 0.16 eV. Previous theoretical and experimental studies[19] of the solvent reorganization energy in liquids provide no evidence to substantiate such a U-shaped temperature dependence. Therefore, either the assumed coupling magnitude of 6 cm^{-1} is inappropriate or the assumption that the coupling magnitude is temperature independent is erroneous. From both these analyses it is clear that a meaningful determination of the coupling magnitude requires more information about the solvent reorganization energy.

As it is not possible to independently measure λ_S for **1**, theoretical estimates and experimental values from related systems need to be considered. Previously, a molecular solvation model, developed by Matyushov,[20] was calibrated[10] to reproduce

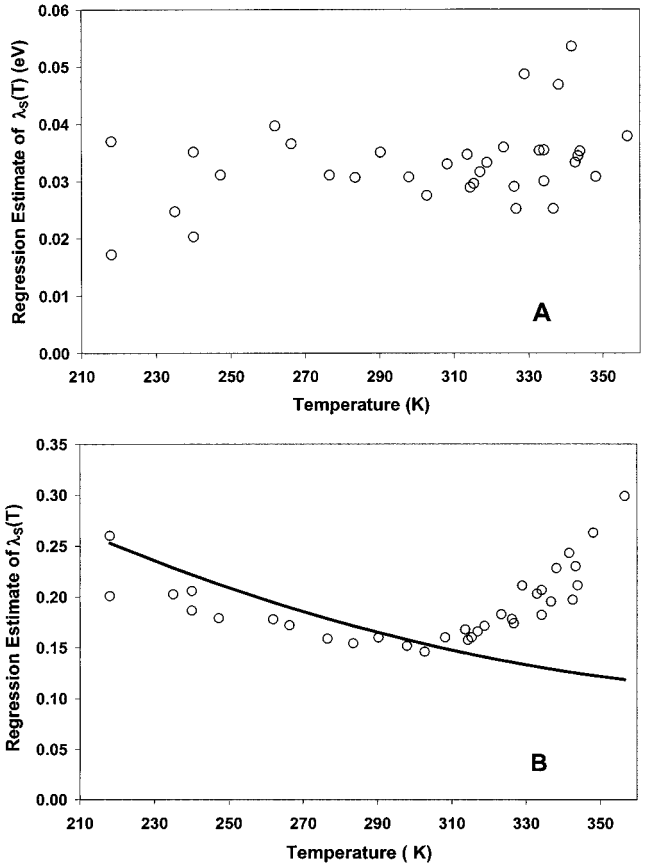

Figure 5. Values of $\lambda_S(T)$ obtained from the experimental rate constant data, eq 2 and an assumed value of $|V|$. The data in panel A were obtained with $|V|$ set to 2.25 cm^{-1}. The data in panel B were obtained by setting $|V|$ equal to 6.0 cm^{-1}. The solid line in panel B shows the $\lambda_S(T)$ prediction from the calibrated Matyushov model.

TABLE 1: Calibrated[10] Solvation Model Predictions of λ_S(295 K), Its First Derivative, and Experimental Values of λ_S(295 K) Determined by Fitting $k_{for}(T)$ and $k_{back}(T)$ Data[a]

solvent	model: $d(\lambda_S(295K))/dT$ (eV/10^3 K)	model: λ_S(295 K)[23] (eV)	expt: λ_S(295 K) (eV)
benzene	−1.1	0.27	0.26
toluene	−1.0	0.24	0.22
cumene	−0.83	0.19	0.17
mesitylene	−0.76	0.17	0.14
TMB	−0.75	0.20	0.16
13DIP	−0.63	0.16	
135TIP	−0.74	0.12	0.01

[a] TMB is 1,2,4-trimethylbenzene, 13DIP is 1,3-di-isopropylbenzene, and 135TIP is 1,3,5-tri-isopropylbenzene.

the experimental values of the charge separation free energy for **1** in alkylated benzene solvents. This calibrated solvation model can be used to predict the magnitude and temperature dependence of the solvent reorganization energy. Table 1 presents these predictions for the solvent reorganization energy and its temperature derivative at 295 K in seven alkylbenzene solvents and compares them to values of λ_S(295 K) that were obtained by fitting experimental rate constant data for **1**.[10,21] The model predicts a monotonic decrease of the solvent reorganization energy with increasing temperature and with increasing alkyl substitution of the solvent molecules. For the first five solvents in Table 1, the model predictions and the experimental values of λ_S(295 K) are in good agreement. Only the regression estimate of λ_S(295 K) in 1,3,5-tri-isopropylbenzene deviates significantly from the model's prediction (see

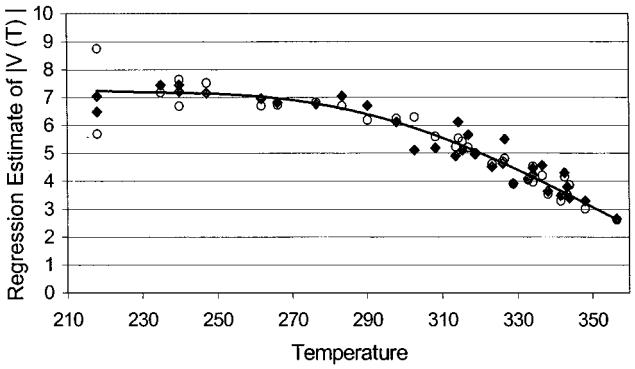

Figure 6. Values of the electronic coupling for **1** in 1,3-di-isopropylbenzene, obtained by fitting the experimental rate constant data using the calibrated Matyushov model to calculate $\lambda_S(T)$, plotted as a function of temperature: (k_{back}, ○), (k_{for}, ◆).

below for an alternative analysis of the kinetic data for **1** in this solvent). The good agreement between the experimental and theoretical values of λ_S in five of the six solvents that are structurally related to 1,3-di-isopropylbenzene suggests that the model's prediction of $\lambda_S = 0.16$ eV at 295 K for this solvent is reasonable. This value is much larger than the λ_S estimate required by assuming $|V| = 2.25$ cm^{-1} but quite close to the value required by assuming $|V| = 6$ cm^{-1}. The solid line in Figure 5B displays the parametrized solvation model prediction of λ_S versus temperature for **1** in 1,3-di-isopropylbenzene.[22] Between 220 and 290 K, the theoretical predictions are slightly larger (by 0.02−0.03 eV) than the $\lambda_S(T)$ values required to reproduce the rate data (circles) for the assumed value of $|V| =$ 6.0 cm^{-1}. These two sets of $\lambda_S(T)$ deviate at higher temperatures.

Both sets of $\lambda_S(T)$ values in Figure 5, panel B, are substantially larger than the experimental $-\Delta_rG$ values, suggesting that the charge separation and charge recombination processes lie in the Marcus normal region at all temperatures. In the Marcus normal region, larger λ_S values reduce the electron-transfer rate constant. The apparent increase of λ_S at temperatures above 310 K (circles, panel B) acts to decrease the transfer rate constant calculated using a temperature independent coupling of 6 cm^{-1}. Given the mobility of solvent molecules and evidence that solvent placement influences coupling magnitude, it is possible that a decrease of the average, effective coupling, rather than an increase of λ_S, may be occurring at temperatures above 310 K. This proposal can be explored by assuming that the parametrized solvation model accurately predicts the magnitude and the temperature dependence of the solvent reorganization energy for **1**. With values for $\lambda_S(T)$, eq 2 may be used to determine the value of the electronic coupling required to reproduce the experimental rate constants at each temperature. The coupling magnitude obtained using this procedure (Figure 6) is relatively constant between 220 and 260 K, 7.2 ± 0.5 cm^{-1}, but decreases by more than 60% between 260 and 350 K.[24] The temperature dependence of k_{for} and k_{back} predicted by this analysis is in very good agreement with the experimental data (Figure 3, dashed lines).

At this point, two models have been advanced to explain the rate data from **1** in 1,3-di-isopropylbenzene. The two models reproduce the rate data using different values and temperature dependences of $|V|$ and λ_S. In the next section, evidence is presented that confirms the validity of λ_S predictions from the calibrated molecular model and the validity of the $|V(T)|$ explanation. Arguments that discount the accuracy of the "inverted" region model are also presented.

IV. Pros, Cons, and Consequences of the Two Explanations

The temperature dependence of the charge separation and charge recombination rate constants for **1** in 1,3-di-isopropylbenzene are well reproduced by both the "inverted region" and the "temperature-dependent electronic coupling" explanations. At low temperatures ($\Delta_rG(CS) < -0.05$ eV), the latter model fits the data slightly more accurately. For both explanations, the solvent reorganization energy is small, less than 0.3 eV. Determining which of the two proposed explanations is correct requires accurate information on the solvent reorganization energy magnitude and its temperature dependence, a task that is not experimentally feasible for **1**. As noted above, a molecular solvation model, which previously was parametrized[10] to reproduce the experimentally determined $\Delta_rG(T)$ data for **1** in a series of alkylbenzene solvents, predicts values of $\lambda_S(295\ K)$ for **1** (ranging from 0.12 to 0.27 eV) that are in good agreement with $\lambda_S(295\ K)$ determined by fitting experimental rate constant data. The model's prediction of $\lambda_S(295\ K)$ for **1** in 1,3-di-isopropylbenzene, 0.16 eV, is significantly larger than the 0.033 eV value required by the "inverted region" explanation. In light of the model's predictive accuracy in the other alkylbenzene solvents, this discrepancy argues against the "inverted region" explanation.

Although **1** lacks detectable CT absorption and emission spectra, some qualitative information about λ_S can be obtained by studying the CT spectra of a related molecule. Compound **2** employs the same donor and acceptor as **1**, connected by an all-trans three-bond bridge, and exhibits CT emission.[25] The donor−acceptor separation in **2** is ∼6 Å, roughly 1 Å smaller than that in **1**. At 295 K, the maximum of the CT emission, Franck−Condon lineshape from **2** appears at 2.19 eV in 1,3-di-isopropylbenzene, 2.12 eV in cumene, and 1.98 eV in benzene.[26] This energy is approximately equal to $\Delta_rG(S_0 \rightarrow CT) - \lambda_S - \lambda_V$ or, equivalently, to $\Delta_rG(S_0 \rightarrow S_1) + \Delta_rG(S_1 \rightarrow CT) - \lambda_S - \lambda_V$. The term $\Delta_rG(S_0 \rightarrow S_1)$ amounts to 3.00 eV for the anthracene chromophore in alkylbenzene solvents and the last term, λ_V, is 0.39 eV. Thus, $\lambda_S - \Delta_rG(S_1 \rightarrow CT)$ for **2** at 295 K is equal to 0.42, 0.49, and 0.63 eV in 1,3-di-isopropylbenzene, cumene, and benzene, respectively.[27] The same quantity, $\lambda_S - \Delta_rG(S_1 \rightarrow CT)$, calculated for **1** using the experimental $\Delta_rG(S_1 \rightarrow CT)$ data and the calibrated solvation model predictions of λ_S (Table 1) amounts to 0.16, 0.24 and 0.37 eV in 1,3-diisopropylbenzene, cumene and benzene, respectively. The variations of $\lambda_S - \Delta_rG(S_1 \rightarrow CT)$ with solvent are nearly identical for **1** and **2**. The offset of 0.26 eV between $\lambda_S - \Delta_rG(S_1 \rightarrow CT)$ for **1** and **2** is consistent with the different charge separation distances of **1** and **2**.[28] The similarity of the solvent dependencies of $\lambda_S - \Delta_rG(S_1 \rightarrow CT)$, for **1** and **2**, in conjunction with the accurate reproduction of the $\Delta_rG(T)$ data for **1** shows that the parametrized molecular model's treatment of solvation by weakly dipolar aromatic solvents and its treatment of solvent structural effects generate meaningful predictions for these anthracene donor, cyclobutenediester electron-transfer systems.[29] Although these arguments do not establish unambiguously the accuracy of the model's $\lambda_S(295\ K)$ predictions, they provide compelling evidence that λ_S for **1** in 1,3-di-isopropylbenzene is larger than 0.033 eV. Accordingly, the "inverted region" explanation is not consistent with the available information on λ_S in 1,3-di-isopropylbenzene.

Another problem with the "inverted region" explanation for **1** in 1,3-di-isopropylbenzene lies in the calculated decrease of the transfer rate when $-\Delta_rG$ is greater than $\lambda_S = 0.033$ eV. This prediction may be an artifact of using a single quantum

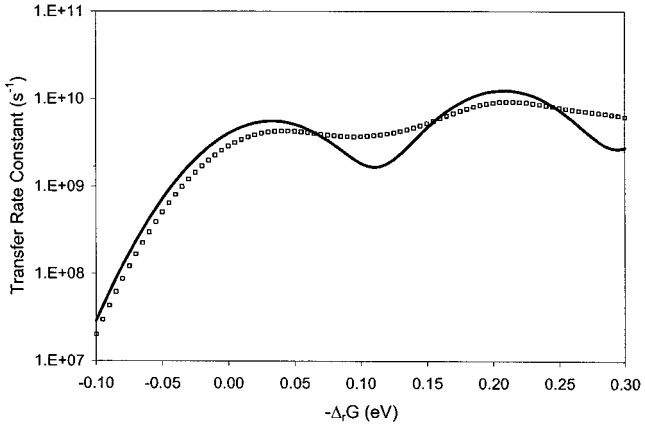

Figure 7. Examples of rate constant versus reaction free energy plots calculated using a one-quantized mode (—) and a two quantized mode (□) model. For both models, $|V| = 6$ cm^{-1}, $\lambda_S = 0.033$ eV, $h\nu_1 = 0.175$ eV, $h\nu_2 = 0.087$ eV, and the total internal reorganization energy is 0.39 eV. For the two quantized mode calculation, the internal reorganization energies are λ_{V1} (0.175 eV mode) = 0.33 eV and λ_{V2} (0.087 eV mode) = 0.06 eV. For the one quantized mode calculation, λ_V (0.175 eV mode) = 0.39 eV.

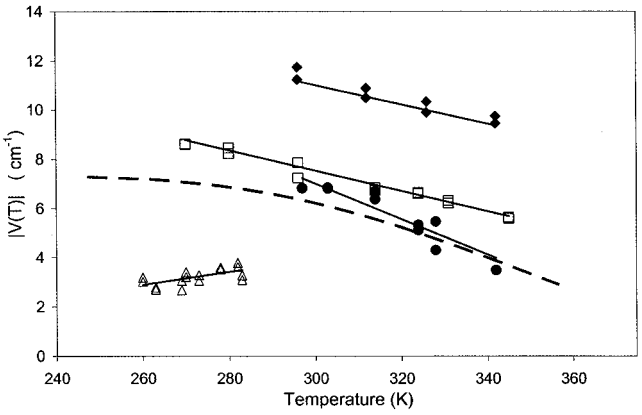

Figure 8. Temperature dependence of the electronic coupling for **1** in benzene (◆), cumene (□), mesitylene (●), and 1,3,5-tri-isopropylbenzene (△), obtained by fitting the experimental rate constant data and using the calibrated Matyushov model to calculate $\lambda_S(T)$. Regression lines are drawn through the data for each solvent. The best fit line to the 1,3-di-isopropylbenzene $|V(T)|$ data (— —) is reproduced from Figure 6.

mode model. If λ_S is significantly smaller than the mode spacing, $h\nu$, eq 2 predicts a significant drop and recovery of the rate constant for $-\Delta_r G$ between λ_S and $\lambda_S + h\nu$ (Figure 7; solid line). A modulation appears in a semilog plot of rate constant versus $-\Delta_r G$, with rate maxima at values of $-\Delta_r G$ that are close to $\lambda_S + nh\nu$.[30] This modulation extends from the "normal" region ($-\Delta_r G < \lambda_S + \lambda_V$), through the peak of the Marcus curve and into the region *traditionally* referred to as inverted ($-\Delta_r G > \lambda_S + \lambda_V$). If a small portion of the internal reorganization energy is associated with a second quantum mode of lower frequency, e.g., $h\nu \sim 700$ cm^{-1}, a two quantum mode rate constant model predicts negligible modulation of the rate constant (Figure 7, squares).[31] Resonance Raman studies of intramolecular CT systems report significant reorganization associated with such intermediate frequency modes in other systems.[32] For **1**, modes involving the donor and acceptor rings likely fall in this range, whereas modes associated with reorganization of the donor methoxy and the acceptor ester groups likely occur at somewhat lower frequency. Thus, more realistic treatments of the internal reorganization within the rate constant calculation predict smaller or negligible reduction of the rate constant when $-\Delta_r G$ is greater than λ_S. This raises additional doubts about the validity of the "inverted region" explanation for the transfer rate data from **1** in 1,3-di-isopropylbenzene.

If the molecular model prediction of λ_S for **1** in 1,3-di-isopropylbenzene is correct, then 1,3,5-tri-isopropylbenzene is the only alkylbenzene solvent for which the molecular model prediction and the experimentally derived value of λ_S differ significantly. The solvent 1,3,5-tri-isopropylbenzene differs from the other alkylbenzenes in that the three bulky isopropyl groups spaced around the aromatic ring prevent facile entry of the solvent's aromatic core into the cleft between the donor and acceptor groups.[8c] Molecular mechanics calculations indicate that only the isopropyl groups from this solvent extend into the cleft. The absence of a "solvent aromatic ring" between the donor and acceptor groups might cause a larger reduction of λ_S, relative to the other solvents, than predicted by the molecular model. The solvation model treats the CT molecule as a point dipole contained within a solvent free cavity. Thus, it does not include "cleft" solvent reorganization energy for any of the solvents.[33] If exclusion of the aromatic core of 1,3,5-tri-isopropylbenzene from the cleft interior is responsible for the 0.11 eV difference between the molecular model prediction and the experimental value (Table 1) of λ_S(295 K), then the molecular model must overestimate the "*extra-cavity*" solvent reorganization energy in all of these alkylbenzene solvents by a comparable amount. This line of reasoning suggests that the solvent reorganization energy attending motion of a single solvent molecule within the cleft, ~0.1 eV, is comparable to the solvent reorganization energy attending motions of all of the solvent molecules surrounding the donor and acceptor groups. Finite difference Poisson−Boltzmann calculations[34] that explicitly account for the shape and presence of a cleft in **1** generate similar values of λ_S whether the solvent is excluded or allowed into the cleft between the donor and acceptor.[35] Thus, exclusion of the aromatic core of 1,3,5-tri-isopropylbenzene from the cleft in **1** is not a likely source for the discrepancy between the calculated and experimental λ_S values.

An alternative explanation for the discrepancy between the molecular model and regression estimate of λ_S for **1** in 1,3,5-tri-isopropylbenzene is that the effective $|V|$ in this solvent is also temperature-dependent. In analogy to the approach employed for **1** in 1,3-di-isopropylbenzene, the magnitude and temperature dependence of the effective coupling for **1** in 1,3,5-tri-isopropylbenzene may be determined by assuming that the molecular model predictions of $\lambda_S(T)$ are correct. The results of this analysis (Figure 8) suggest that the effective coupling for **1** in 1,3,5-tri-isopropylbenzene *increases* with temperature, from 2.9 cm^{-1} at 260 K to 3.5 cm^{-1} at 283 K. A positive value of $d|V|/dT$ provides a simple explanation for the experimental observation that *both* k_{for} *and* k_{back} *increase with temperature* in this solvent. The magnitude of the coupling obtained from this analysis is larger than the value of 1.0 cm^{-1} previously obtained with the assumption of a temperature independent coupling magnitude and a regression estimate of λ_S(295 K) = 0.01 eV. It is not surprising that a larger magnitude of $|V|$ is obtained when larger values of λ_S are used in the analysis (Figure 4). Even with this increase, the effective coupling for **1** in 1,3-di-isopropylbenzene is still more than 2-fold larger than in 1,3,5-tri-isopropylbenzene (260 K < T < 283 K). As was suggested previously, increased steric bulk about the periphery of the solvent's aromatic π system results in less effective solvent-mediated coupling.

Figure 8 shows the $|V(T)|$ values that are obtained for the other alkylbenzene solvents when the solvation model's predic-

tions for the temperature-dependent reorganization energy are assumed to be correct. The effective coupling magnitude, derived from the rate data and the molecular model $\lambda_S(T)$, decreases with increasing temperature in the solvents benzene, cumene, and mesitylene. The diminution is greatest for mesitylene, for which the coupling magnitude and temperature dependence are similar to that for **1** in 1,3-di-isopropylbenzene. The steep decrease of the coupling in mesitylene provides an explanation for the failure of the previous analysis,[10] which assumed temperature independent coupling magnitudes, to reproduce the experimentally observed steep decrease of k_{for} and k_{back} at temperatures above 315 K. The temperature derivative of the effective coupling in benzene and cumene, -0.04 cm^{-1} K^{-1}, is about half as large as that for mesitylene. For the five alkylbenzene solvents, the effective coupling magnitudes at 295 K are 12 cm^{-1} in benzene, 7.4 cm^{-1} in cumene, 6.8 cm^{-1} in mesitylene, 6.3 cm^{-1} in 1,3-di-isopropylbenzene, and 3.9 cm^{-1} in 1,3,5-tri-isopropylbenzene.[36] With the exception of the last solvent, these magnitudes are within 20% of the values derived previously from analyses premised on temperature independent coupling.[10]

The structure and the number of alkyl groups on the periphery of the solvents' aromatic ring alter the electronic coupling magnitude for **1**. The alkyl groups have a minor effect on the aromatic π system's energy levels. They do influence the probabilities of locating the aromatic π system in positions that offer simultaneous overlap with the donor and the acceptor. Theoretical investigations confirm that such simultaneous overlap is necessary for a coupling pathway constituted by a single solvent molecule to be effective.[5e] For a C-shaped molecule such as **1**, simultaneous overlap and significant coupling are realized by placement of the solvent's aromatic π system within the 7 Å wide cleft, directly between the donor and acceptor groups.[37] The observed dependence of **1**'s electronic coupling magnitude on the identity of the alkyl groups around the aromatic ring and on temperature can be explained in terms of solvent entry into this cleft. A benzene molecule readily accesses "in-cleft" solvent configurations that provide significant, simultaneous overlap of the solvent with the donor and the acceptor of **1**. For many of these "in-cleft" configurations of the benzene, substituting a peripheral H atom by an alkyl group introduces steric repulsion between the alkyl group and **1**. This repulsion disfavors solvent configurations with the aromatic core situated deeply within the cleft. Solvent configurations in which the (bulky) alkyl groups are farther from the cleft walls and edges are more probable. The latter configurations offer smaller simultaneous overlap of the donor and acceptor with the solvent π orbitals and, therefore, smaller electronic coupling. Larger and/or more numerous alkyl groups more severely reduce the probability of solvent configurations with large overlap and significant coupling. This explains the observed reduction of coupling magnitude with increasing alkyl substitution of the solvent.

Each "in-cleft" solvent configuration affords a unique coupling magnitude. As solvent molecules move within and out of the cleft, the donor−acceptor coupling magnitude fluctuates. The probability of an electron-transfer event is very small during any single initial state−final state level crossing (nonadiabatic transfer). As a result, each molecule of **1** samples a "large number" of solvent configurations before there is significant probability that the ensemble of excited states has undergone electron transfer. Rapid interconversion among solvent−**1** configurations, compared to the electron-transfer rate, generates experimental charge separation dynamics that are well reproduced by a single electron-transfer rate constant with an effective coupling magnitude that is a root-mean-square average of the individual coupling magnitude, $(V_j)^2$, in each possible configuration, $|V| = [\sum_j p_j (V_j)^2]^{1/2}$. The probability of each configuration, p_j, is determined by its free energy and by the temperature. The probability of each solvent−**1** configuration changes differently with temperature, thus altering the distribution of mediating configurations and the average value of the coupling. This provides an explanation for the temperature dependence of the observed electronic coupling.

SCHEME 1

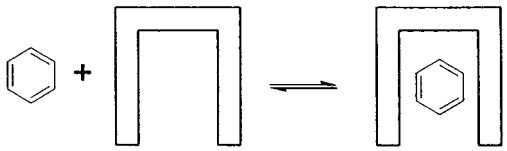

The different signs of $d|V|/dT$ for **1** in benzene and 1,3,5-tri-isopropylbenzene may be attributed to the most prevalent "state" of the cleft in each solvent. For example, benzene readily fits within the cleft of **1**, and the equilibrium (see Scheme 1) should be characterized by a negative $\Delta H°$ and a negative $\Delta S°$.[38] Upon increasing the temperature, the equilibrium shifts toward "empty-cleft" configurations. Because the "in-cleft" solvent configurations provide larger electronic coupling than the "empty cleft" configurations, the effective coupling magnitude in benzene decreases as the temperature increases. The rather shallow dependence of $|V|$ on temperature for **1** in benzene and cumene suggests that "in-cleft" configurations predominate throughout the investigated temperature ranges. The steeper dependence of $|V|$ on temperature for **1** in mesitylene and in 1,3-di-isopropylbenzene indicate more significant conversion from predominantly "in-cleft" to "empty-cleft" configurations. The solvent 1,3,5-tri-isopropylbenzene presents a different situation. Steric repulsion between the isopropyl groups and **1** results in a positive enthalpy for formation of "in-cleft" solvent configurations in which the solvent's aromatic core is between the donor and acceptor. These configurations provide larger electronic coupling, but $\Delta G°$ for their formation is positive (i.e., the equilibrium constant for their formation is less than 1). Higher temperature increases the fraction of these higher free energy, larger coupling, "in-cleft" configurations, and enhances the effective coupling magnitude. Given the excellent correspondence between the experimental rate data for **1** and the rates calculated using the parametrized molecular model in a variety of alkylbenzene solvents, variation of the solvent-mediated electronic coupling magnitude with temperature is a likely explanation for the unusual electron-transfer kinetics of **1** in 1,3-di-isopropylbenzene.

V. Conclusion

The charge separation and charge recombination rate constants for **1** in 1,3-di-isopropylbenzene increase, plateau, and then decrease when plotted against temperature or the experimentally determined reaction free energy change. Within the framework of a single quantum-mode, semiclassical electron transfer rate expression, the origin of this rate behavior lies in the temperature dependence of the solvent reorganization energy and/or of the electronic coupling. Two explanations of the kinetic behavior have been advanced. The experimental data can be simulated using a small and temperature-independent solvent reorganization energy or a temperature-dependent electronic coupling magnitude. In the first scenario, the variation of the reaction driving force with temperature shifts the reactions

between the Marcus normal and the Marcus inverted regions and is responsible for the highly curved rate plots. Between 210 and 360 K, $\Delta_r G$ for the charge separation and charge recombination reactions are insufficient to populate "products" with one or more quanta of vibrational energy.[39] Thus, the electron transfer rate constant in the normal and inverted regions decreases comparably as the reaction free energy shifts away from the optimum value. For this explanation to apply, there cannot be significant vibrational reorganization (energy) associated with modes in the 400−700 cm^{-1} range. The solvent reorganization energy would also need to be extremely small and unusually temperature-independent. Additionally, there are very few examples of charge separation reactions (neutral reactant → zwitterionic product) that exhibit rate versus $\Delta_r G$ profiles consistent with the Marcus inverted region.[40] Although many explanations have been advanced to justify the paucity of examples, invoking the inverted region to explain the rate constant data from **1** finds little if any precedent. This would also be the first example of a charge separation reaction in nonpolar solvents lying in the Marcus inverted region.

The alternative explanation for the kinetic data posits that the electronic coupling magnitude varies with temperature. Between 290 and 350 K, the effective coupling for **1** decreases 60% in 1,3-di-isopropylbenzene, 50% in mesitylene, and 30% in cumene. The extensive curvature in the bridge of **1** requires an appropriately placed solvent molecule within the cleft between the donor and acceptor to mediate the electronic coupling. The probability of appropriate solvent placement and the efficacy of solvent-mediated coupling both vary with solvent structure and temperature. Although there are theoretical studies that support the feasibility of temperature-dependent, solvent-mediated coupling magnitudes,[5,41] there is not yet *direct* evidence to confirm this explanation. The evidence in this manuscript is indirect, relying on a parametrized solvation model to provide accurate predictions of the solvent reorganization as a function of solvent structure and temperature. More direct investigation of the temperature dependence in solvent-mediated electronic coupling is clearly desirable. In summary, the experimental rate constant behavior for **1** in a number of alkylbenzene solvents is most reasonably explained by invoking a significant temperature dependence for the solvent-mediated, electronic coupling magnitude. Temperature-dependent electronic coupling may influence electron-transfer dynamics in any system where the composition or the structure of the coupling pathway fluctuates significantly.

Acknowledgment. This work was supported in part by the National Science Foundation (Grants CHE-9708351, 0108945 (MBZ) and CHE-0111435 (DHW)).

References and Notes

(1) (a) Gould, I. R.; Young, R. H.; Moody, R. E.; Farid, S. *J. Phys. Chem.* **1991**, *95*, 2068. (b) Gould, I. R.; Young, R. H.; Mueller, L. J.; Albrecht, A. C.; Farid, S. *J. Am. Chem. Soc.* **1994**, *116*, 8188.

(2) (a) Winkler, J. R.; Di Bilio, A. J.; Farrow, N. A.; Richards, J. H.; Gray, H. B. *Pure Appl. Chem.* **1999**, *71*, 1753. (b) Casimiro, D. R.; Beratan, D. N.; Onuchic, J. N.; Winkler, J. R.; Gray, H. B *Adv. Chem. Ser.* **1995**, *246*, 471. (c) Miller, J. R.; Beitz, J. V.; Huddleston, R. K. *J. Am. Chem. Soc.* **1984**, *106*, 5057.

(3) (a) Hush, N. S. *Coord. Chem. Rev.* **1985**, *64*, 135. (b) Oliver, A. M.; Paddon-Row, M. N.; Kroon, J.; Verhoeven, J. W. *Chem. Phys. Lett.* **1992**, *191*, 371. (c) Morais, J.; Hung, R. R.; Grabowski, J. J.; Zimmt, M. B. *J. Phys. Chem.* **1993**, *97*, 13138. (c) Bixon, M.; Jortner, J.; Verhoeven, J. W. *J. Am. Chem. Soc.* **1994**, *116*, 7349.

(4) (a) Closs, G. L.; Miller, J. R. *Science* **1988**, *240*, 440. (b) Paddon-Row, M. N. *Acc. Chem. Res.* **1994**, *27*, 18. (c) Sachs, S. B.; Dudek, S. P.; Hsung, R. P.; Sita, L. R.; Smalley, J. F.; Newton, M. D.; Feldberg, S. W.; Chidsey, C. E. D. *J. Am. Chem. Soc.* **1997**, *119*, 10563. (d) Winkler, J. R.; Gray, H. B. *J. Biol. Inorg. Chem.* **1997**, *2*, 399. (e) Lewis, F. D.; Letsinger, R. L. *J. Biol. Inorg. Chem.* **1998**, *3*, 215. (f) Davis, W. B.; Svec, W. A.; Ratner, M. A.; Wasielewski, M. R *Nature* **1998**, *396*, 60.

(5) (a) Chohan, K. K.; Jones, M.; Grossmann, J. G.; Frerman, F. E.; Scrutton, N. S.; Sutcliffe, M. J. *J. Biol. Chem.* **2001**, 276, 34142. (b) Jones, G. A.; Carpenter, B. K.; Paddon-Row, M. N. *J. Am. Chem. Soc.* **1999**, *121*, 11171. (c) Xie, Q.; Archontis, G.; Skourtis, S. S. *Chem. Phys. Lett.* **1999**, *312*, 237. (d) Balabin, I. A.; Onuchic, J. N. *Science* **2000**, *290*, 114. (e) Cave, R. J.; Newton, M. D.; Kumar, K.; Zimmt, M. B. *J. Phys. Chem.* **1995**, *99*, 17501. (f) Castner, E. W., Jr.; Kennedy, D.; Cave, R. J. *J. Phys. Chem. A* **2000**, *104*, 2869.

(6) (a) Davis, W. B.; Ratner, M. A.; Wasielewski, M. R. *J. Am. Chem. Soc.* **2001**, *123*, 7877. (b) Graige, M. S.; Feher, G.; Okamura, M. Y. *Proc. Natl. Acad. Sci. U.S.A.* **1998**, *95*, 11679. (c) Hoffman, B. M.; Ratner, M. A. *J. Am. Chem. Soc.* **1987**, *109*, 6237. (d) Intermolecular electron-transfer reactions are influenced by the dependence of electronic coupling on donor−acceptor separation and the nature of the intervening medium. See ref 5f.

(7) Fluctuations of rigid bridge mediated coupling magnitudes are small compared to the mean coupling matrix element in systems where the donor acceptor interaction is not symmetry forbidden (see the last column (H_{CR}) of Table 1 for **1** in ref 5e. In systems where the donor−acceptor interaction is symmetry forbidden, the mean coupling value is small. Distortions of the molecular structure can generate coupling magnitudes that are larger than the mean value. See the sixth column (H_{CS}) of Table 1 for **1** in ref 5e.

(8) (a) Lawson, J. M.; Paddon-Row, M. N.; Schuddeboom, W.; Warman, J. M.; Clayton, A. H. A.; Ghiggino, K. P. *J. Phys. Chem.* **1993**, *97*, 13099. (b) Kumar, K.; Lin, Z.; Waldeck, D. H.; Zimmt, M. B. *J. Am. Chem. Soc*. **1996**, *118*, 243. (c) Read, I.; Napper, A.; Kaplan, R.; Zimmt, M. B.; Waldeck, D. H. *J. Am. Chem. Soc*. **1999**, *121*, 10976. (d) Lokan, N. R.; Paddon-Row, M. N.; Koeberg, M.; Verhoeven, J. W. *J. Am. Chem. Soc*. **2000**, *122*, 5075. (e) Kaplan, R. W.; Napper, A. M.; Waldeck, D. H.; Zimmt, M. B. *J. Am. Chem. Soc.* **2000**, *122*, 12039.

(9) The following citation describes the pressure dependence of electronic orbital overlap in hydrogen bonds: Li, H.; Yamada, H.; Akasaka, K.i; Gronenborn, A. M. *J. Biomol. NMR* **2000**, *18*, 207.

(10) Read, I.; Napper, A.; Zimmt, M. B.; Waldeck, D. H. *J. Phys. Chem. A* **2000**, *104*, 9385.

(11) Napper, A. M.; Read, I.; Kaplan, R.; Zimmt, M. B.; Waldeck, D. H. *J. Phys. Chem. A* **2002**, *106*, in press.

(12) The rate constant, k_{rec}, comprises two distinct electron-transfer processes; conversion of the CT state to the molecule's ground singlet state and to the molecule's lowest energy triplet state. This is of no consequence to the current investigation.

(13) (a) Kumar, K.; Tepper, R. J.; Zeng, Y.; Zimmt, M. B. *J. Org. Chem.* **1995**, *60*, 4051. (b) Kaplan, R. Ph.D. Thesis, Brown University, Providence, RI, 2001.

(14) (a) Zeglinski, D. M.; Waldeck, D. H. *J. Phys. Chem.* **1988**, *92*, 692. (b) O'Connor, D. V.; Phillips, D. *Time Correlated Single Photon Counting*; Academic Press: New York, 1984.

(15) The fluorescence decay of **1** is fit to the biexponential form: $I(t) = a_+e^{-k_+t} + (1 - a_+)e^{-k_-t}$. The forward electron-transfer rate constant k_{for} is obtained from $k_{for} = a_+(k_+ - k_-) - k_f + k_-$, and the reverse electron-transfer rate constant k_{back} is obtained from $k_{back} = [(k_+ - k_-)^2 - (2k_f + 2k_{for} - k_+ - k_-)^2]/4k_{for}$. See the text for determination of k_f.

(16) The best fit equation is $\Delta_r G(eV) = 5.2451 \times 10^{-6}T^2 - 2.0156 \times 10^{-3}T + 1.2979 \times 10^{-1}$. The temperature is in units of K.

(17) Jortner, J. *J. Chem. Phys.* **1976**, *64*, 4860.

(18) (a) Zeng, Y.; Zimmt, M. B. *J. Phys. Chem.* **1992**, *96*, 8395. (b) Kumar, K.; Kurnikov, I.; Beratan, D.; Waldeck, D.; Zimmt, M. B. *J. Phys. Chem. A* **1998**, *102*, 5529.

(19) (a) Vath, P.; Zimmt, M. B.; Matyushov, D. V.; Voth, G. A. *J. Phys. Chem. B* **1999**, *103*, 9130. (b) Vath, P.; Zimmt, M. B. *J. Phys. Chem. A* **2000,** *104*, 2626. (c) Derr, D. L.; Elliott, C. *J. Phys. Chem. A* **1999**, *103*, 7888. (d) Matyushov, D. V. *Chem. Phys*. **1993**, *174*, 199. (e) Cortés, J.; Heitele, H.; Jortner, J. *J. Phys. Chem*. **1994**, *98*, 2527. (f) Evidence of increasing λ_S with decreasing temperature for bacterial reaction centers is presented in Ortega, J. M.; Mathis, P.; Williams, J. C.; Allen, J. P. *Biochemistry* **1996**, *35*, 3354.

(20) Matyushov, D. V.; Voth, G. A. *J. Chem. Phys*. **1999**, 111, 3630.

(21) The only other fitting parameter in these analyses was $|V|$, which was assumed to be temperature-independent.

(22) Over small temperature ranges, the predicted λ_S appear to vary linearly with temperature. Over larger temperature ranges (140 K for 13DIP), curvature in the $\lambda_S(T)$ plots are evident.

(23) The predicted values in column 3 of Table 1 are larger than previously reported in ref 10. A numerical error in a subroutine was responsible. The results of the corrected code have been checked with code kindly provided by Professor Matyushov.

(24) The line in Figure 6 is a polynomial fit to this derived $|V(T)|$ data. A polynomial fit yields $|V(T)| = 2.257 \times 10^{-8}T^4 - 2.630 \times 10T^3 + 1.106 \times 10^{-2}T^2 - 2.014 \times 10T + 1.423 \times 10^2$. The temperature is in units of K and $|V|$ is in cm^{-1}.

(25) Compound **2** in the current manuscript is the same as compound **8** in reference 18a.

(26) (a) The line shape of a CT emission band includes contributions from the frequency dependence of the transition moment in addition to the frequency dependence of the Franck−Condon factors.[26b] After correcting for the frequency dependence of the transition moment, the Franck−Condon line shape remains. The energy corresponding to the maximum of this line shape is reported in the text. (b) Marcus, R. A. *J. Phys. Chem.* **1989**, *93*, 3078. (c) It is not possible to extract unique values of λ_S and $\Delta_r G$ for compound **2** in alkylbenzene solvents. Impurity emissions obscure the blue side of these spectra, making a unique determination of $\Delta_r G$ impossible. The absence of detectable CT absorption bands eliminates a second route to unique $\Delta_r G$ determination. Consequently, there is substantial, correlated uncertainty in values of $\Delta_r G$ and λ_S obtained by fitting the CT emission line shape.

(27) Both λ_S and $-\Delta_r G(S_1 \rightarrow CT)$ are positive quantities that increase with increasing (nuclear) solvation. As a result, solvation differences provided by various alkylbenzene solvents reinforce, rather than cancel, in the term $\lambda_S - \Delta_r G(S_1 \rightarrow CT)$.

(28) In alkylbenzene solvents, the Coulomb interaction between the donor cation and acceptor ion amounts to 14.4 eV Å/(2.3 × 7.1 Å) = 0.88 eV for **1** and 14.4 eV Å/(2.3 × 5.7 Å) = 1.10 eV for **2**. The difference of these two values, 0.22 eV, is about the same as the 0.26 eV difference between the $\lambda_S - \Delta_r G(S_1 \rightarrow CT)$ values presented for **1** and **2**.

(29) Comparison of the magnitude and solvent dependence of λ_S for **1** and **2** would be particularly informative. It is not possible to extract accurate values of λ_S from the CT emission spectra.[26c]

(30) Ulstrup, J.; Jortner, J. *J. Chem. Phys.* **1975**, *63*, 4358.

(31) Figure 7 shows that the one quantum mode and two quantum mode models predict different rate constant dependence on reaction free energy for $-\Delta_r G > \lambda_S$. The two models predict comparable rate constant magnitudes and dependencies for $-\Delta_r G < \lambda_S$, however. Use of the two quantum model with $|V| = 7$ cm^{-1} and the parameters in Figure 7 yields rate constants that are indistinguishable from rate constants predicted using $|V| = 6$ cm^{-1} and the one quantum mode model in the range $-\Delta_r G < \lambda_S$. This demonstrates that electronic coupling magnitudes extracted from rate constant data in the Marcus normal region depend weakly on the model used to simulate the vibrational Franck−Condon factors. For further discussion of the influence of zero, one, and multi quantum mode models on Franck−Condon factors and extracted values of the electronic coupling, see refs 18b and 32d.

(32) (a) Hupp, J. T.; Williams, R. D. *Acc. Chem. Res.* **2001**, *34*, 808. (b) Hogiu, S.; Dreyer, J.; Pfeiffer, M.; Brzezinka, K.-W.; Werncke, W. *J. Raman. Spectrosc.* **2000**, *31*, 797. (c) Godbout, J. T.; Zuilhof, H.; Heim, G.; Gould, I. R.; Goodman, J. L.; Dinnocenzo, J. P.; Kelley, A. M. *J. Raman Spectrosc*. **2000**, *31*, 233. (d) Lilichenko, M.; Tittelbach-Helmrich, D.; Verhoeven, J. W.; Gould, I. R.; Myers, A. B. *J. Chem. Phys.* **1998**, *109*, 10958.

(33) If reorganization of the cleft solvent makes significant contribution to λ_S, the agreement between the molecular model prediction and the experimental results (Table 1) is fortuitous and suggests that the parametrization of the molecular model overestimates the extra-cavity solvation of **1**.

(34) (a) Sharp, K.; Honig, B. *Annu. Rev. Biophys. Biophys. Chem.* **1990**, *19*, 301. (b) Sitkoff, D.; Sharp, K. A.; Honig, B. *J. Phys. Chem.* **1994**, *98*, 1978. (c) Zhang, L. Y.; Frieser, R. A. *J. Phys. Chem.* **1995**, *99*, 16479.

(35) The finite-difference Poisson−Boltzmann calculations indicate that exclusion of the solvent from the cleft of **1** reduces the solvent reorganization energy by less than 10%. See ref 18b.

(36) The value of $|V(295\ K)|$ provided for 1,3,5-tri-isopropylbenzene is a linear extrapolation of the results obtained at lower temperatures.

(37) An alkyl group within the cleft provides smaller donor−acceptor electronic coupling than an aromatic ring in the cleft because the lowest energy superexchange state, D^+S^-A, has the "transferring" electron localized on the aromatic ring.

(38) (a) Dispersion and electrostatic interactions[38b] between the anthracene, benzene, and the alkene diester generate a negative enthalpy change for solvent entry. Solvent "complexation" with **1** results in a reduction of translational entropy relative to two, independently diffusing molecules. (b) Tsuzuki, S.; Honda, K.; Uchimaru, T.; Mikami, M.; Tanabe, K. *J. Am. Chem. Soc.* **2002**, *124*, 104.

(39) According to the best fit analysis, approximately 10% of the charge recombination products are formed with one quantum of vibrational energy when the temperature reaches 360 K.

(40) (a) Smitha, M. A.; Prasad, E.; Gopidas, K. R. *J. Am. Chem. Soc.* **2001**, *123*, 1159. (b) Prasad, E.; Gopidas, K. R. *J. Am. Chem. Soc*. **2000**, *122*, 3191.

(41) (a) Segal, D. A; Nitzan, A.; Davis, W. B.; Wasielewski, M. R.; Ratner, M. A. *J. Phys. Chem. B* **2000**, *104*, 3817. (b) Ashkenazi, G.; Kosloff, R.; Ratner, M. A. *J. Am. Chem. Soc*. **1999**, *121*, 3386. (c) Tang, J. *J. Chem. Phys.* **1993**, *98*, 6263.